

Proceedings Article

Drive and receive coil design for a human-scale MPI system

Eli Mattingly ^{a,b,c} · Erica E. Mason ^b · Monika Śliwiak ^b · Lawrence L. Wald ^{a,b,c*}

^aMassachusetts Institute of Technology, Cambridge, MA, USA

^bMartinos Center for Biomedical Imaging, Massachusetts General Hospital, Charlestown, MA, USA

^cHarvard Medical School, Boston, MA, USA

*Corresponding author, email: LWald@mgh.harvard.edu

© 2022 Mattingly *et al.*; licensee Infinite Science Publishing GmbH

This is an Open Access article distributed under the terms of the Creative Commons Attribution License (<http://creativecommons.org/licenses/by/4.0>), which permits unrestricted use, distribution, and reproduction in any medium, provided the original work is properly cited.

Abstract

Scaling MPI imaging hardware to image a human head presents challenges for the primary drive and receive coils. The larger imaging volume necessitates increased inductance, power delivery, and large physical sizes. Here, we present human-head scale drive and receive solenoid coils in a split gradiometer configuration designed for a mechanically-rotating field-free line MPI system. The design efficiency allows for 8 mT drive fields (at ~26 kHz) from the water-cooled drive coil using an amplifier providing ~40 A RMS and ~120 V RMS into the drive filter. The geometric decoupling between the drive and Rx coil of the gradiometer pair is -52 dB.

I. Introduction

We have designed a human-scale drive and receive coil gradiometer assembly for a mechanically rotating field-free line (FFL)-based MPI system (~20 cm field of view). Because the end application of the system is functional neuroimaging of small changes in a MPI time-series, temporal stability is a critical parameter. Our target is less than 1% magnitude drift and 3 degrees phase drift. For simplicity, both the drive and receive coils are solenoids. To avoid having an excessively long patient bore housing both halves of the gradiometer, the design is split with half of the drive solenoid and half of the receive solenoid in the patient bore and the other half (with opposite relative polarity) in a matching conductive bore geometry on the floor near the gantry (see Fig. 1). A mechanical adjustment of the floor-mounted Rx coil relative to its drive solenoid allows nulling of the drive system's induced voltage in the receive system as previously mentioned [1]. This reference also discusses other techniques of feed-through mitigation. The drive system is powered

by an AE Techron 8512 amplifier (Elkhart, IN), which produces the ~40 A RMS in the apparent 3 Ohm load (tuned drive coil plus impedance transformation and filter) to create an 8 mT peak drive field.

II. Methods and materials

II.1. Drive Coil

The drive coil design goal was an 8 mT drive field near 26 kHz with an inner winding diameter of 27 cm within a 40 cm diameter shielded patient bore tube. The drive amplitude was picked to balance peripheral nerve stimulation concerns and tracer performance. The drive coil uses 4 mm diameter copper wire with a 2 mm dia. hole for water cooling. This wire was picked because despite the higher losses compared to Litz wire at 26 kHz, the hollow conductors have excellent thermal contact with the water coolant. This enables better temperature stability at the cost of drive efficiency. The temperature drift in the case of hollow wires will also have a much faster

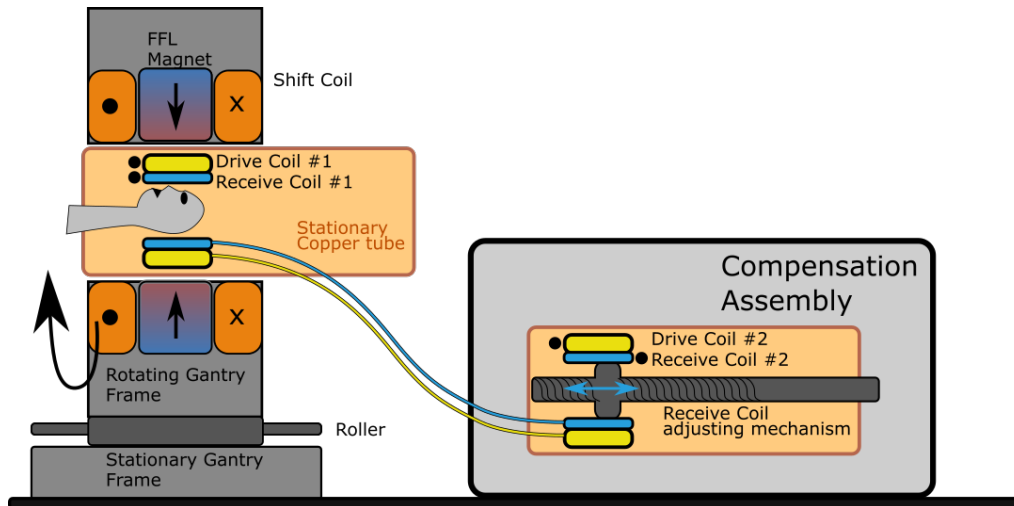


Figure 1: The general arrangement of the split-gradometer drive/receive assemblies. The patient's head is inside one drive/Rx pair within the rotating FFL gantry, and the second drive/Rx pair is wired in series and mounted on the floor nearby. The relative winding sense in this second pair is reversed from the patient's coils in order to provide cancellation of the induced drive voltage in the Rx system (drive feed-through).

time constant and be much more easily predicted and controlled than flood-cooling Litz wires. The wire wall thickness was based on skin depth ($\sim 400 \mu\text{m}$ at 26 kHz), and proximity simulations that were run using FEMM 4.2 [2]. The cooling capacity was determined by using Eqn. 13 in Ref. [3] with the input condition being the pressure capacity of an available pump (Approx. 60 PSI on the final system).

We examined different turn configurations with the given wire size, and chose a 54 turn, 4 layer design for each of the two halves of the split drive coil. The winding configuration (cross-section) is shown in Fig. 2. The spacing between the conductor surfaces is always greater than 2 mm. Each drive coil half (on-patient unit and compensation assembly) was split into 3 winding modules to allow distributed series capacitance tuning so that the voltage drop across each capacitor was within the voltage limit of the Celems CSM nano (Jerusalem, Israel) (1600 V RMS limit for the 200 nF configuration). Due to eddy current heating in the capacitors, they were mounted at the end of the bore where the AC field is a much lower amplitude. The modules also allowed parallelization of the water cooling paths, increasing heat removal efficiency. The modules are 3D printed to ensure consistent dimension and wire spacing. The overall inductance and resistance was calculated to be $590 \mu\text{H}$ and 1.20 Ohms at 26 kHz for each of the two halves and requires a drive current of ~ 60 Amps peak to achieve the 8 mT peak target field. The voltage across each full tuned coil is 75 V peak at full current. The proximity effect losses of different winding patterns were simulated as a function of frequency for multiple combinations of layers and turns per layer in the module. The spacing between the wires was decreased (improving field generation per amp by

allowing for more turns) until the proximity effects dominated skin-effect conductor losses at 26 kHz. The chosen design is shown in Fig. 2, and a photograph of the drive modules are seen in Figure 3. With 60 A Pk, each drive coil assembly dissipates 1.9 kW and another 260 W are dissipated in the tube.

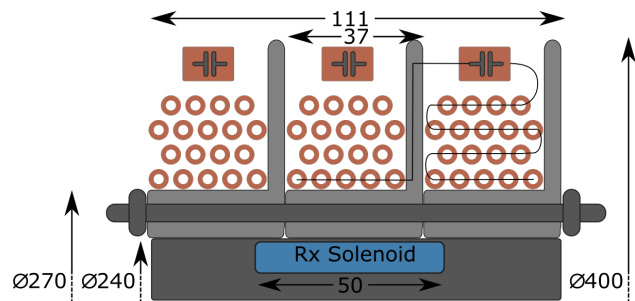


Figure 2: Illustration (not to scale) of the cross-section of the drive coils showing wire spacing. Black line indicated winding pattern. All dimensions are in mm.

II.II. Receive Coil

The Rx solenoid is a head-sized oval cross section (118 mm major radius, 83 mm minor radius and 50 mm length) to increase sensitivity and decrease inductance (relative to circular). It uses 42 turns of Litz wire (195 x 42 AWG Type 2, New England Wire Technologies, Lisbon, NH) in each half, wound on a 3D printed former. The former mounts in the center of the drive coil half, and the floor-mounted compensation unit (which does not contribute to sample signal) contained a screw mechanism controlling relative drive-Rx placement to minimize

drive feed-through.

The topology of the Rx filter is a fully differential notch, similar to ref. [4], and includes a transformer (N87, B64290A0699, TDK, Tokyo, JP) to couple it to the preamp. The value of the shunt inductors and magnetizing inductance must be sufficiently large relative to the Rx coil inductance to avoid voltage division in the filter.

An in-house preamp is used, which facilitates stacking the input stage to change the relative contributions of current and voltage noise as in [5]. We utilized the ADA4807-4 for its compact layout. For the case of 12 parallel opamps there will theoretically be $2.4 pA/\sqrt{Hz}$ current noise and $890 pV/\sqrt{Hz}$ voltage noise. Using JFETs (e.g. 2SK2394-7) in parallel as a common-source preamp as in [6] may provide lower noise, but the high input capacitance (10 pF each, not including miller capacitance) and less certain linearity motivated our choice.

III. Experiments

To test the coolant flow calculations, we used a single module on the bench and connected it to a submersible pump (Little Giant NK-2) in a basin at the same height with a 5.2 PSI maximum pressure and measured the out-flow rate, and then compared to our simulations. For the gradiometer cancellation, we compared the induced voltage in a single Rx coil to the summation of the two when the net voltage was at a minimum. The figure of merit for cancellation is defined as: $20 \log_{10} \left(\frac{V_{single}}{V_{both}} \right)$

IV. Results

For a 5.2 PSI pump, the expected flow rate was 1.1 mL per second, and we measured 0.84 mL per second. Using the same equations with a larger 60 PSI pump, the expected steady-state temperature rise is 30 deg. C at 8 mT peak (100 % duty cycle). The discrepancy may be due to the necessary connectors and bends of the tubing, but will not impact cooling strategy. Simulations done in FEMM 4.2 [2] projected we achieve 0.14 mT/Amp, have an inductance of 590 μ H and a 1.20 Ohms resistance at 26.4 kHz for each of the drive coils. We measured 592 μ H in series with 63.2 nF and 1.26 Ohms at 26 kHz. The Rx coil measures 464 μ H and a 2.45 Ohms at 100 kHz. With the gradiometer set-up we were able to achieve 52 dB feed-through attenuation.

V. Discussion & Conclusion

We describe drive/Rx split gradiometer pair for human brain imaging. The drive coil uses a modular design, water cooling and a winding pattern optimizing proximity effect losses. The design prioritizes temporal stability and manufacturing ease over efficiency. We show that the

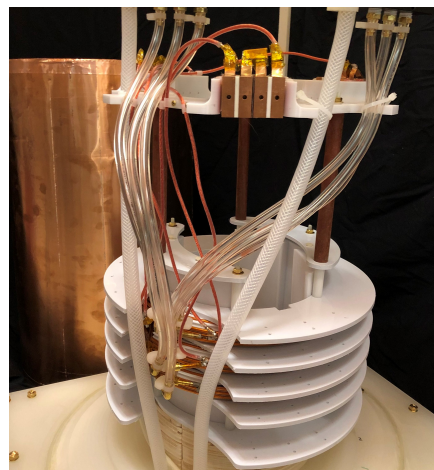


Figure 3: Photograph of the drive coil showing three “modules” separated by spacers. Each drive module has 18 turns and 6 capacitors in a series/parallel combination to equate to 200 nF for a maximum allowable voltage and current of 1600 V RMS, over 100 A RMS respectively. The capacitors are mounted at the end of the bore to prevent eddy current heating.

coolant flow can be predicted with sufficient accuracy. Future work will incorporate a transverse saddle Rx coil into the design.

Acknowledgments

We thank Alex Barksdale and John Drago for their helpful conversation regarding the MPI system and Konstantin Herb for his help on the initial designs.

Author’s statement

Research funding: Funding for the work comes from NIBIB U01EB025121, and NSF GRFP 1122374. Authors state no conflict of interest.

References

- [1] M. Graeser, T. Knopp, M. Grüttner, T. F. Sattel, and T. M. Buzug. Analog receive signal processing for magnetic particle imaging. *Medical Physics*, 40(4), 2013, doi:10.1118/1.4794482.
- [2] D. Meeker, Finite Element Method Magnetics Version 4.2 User’s Manual, 2015.
- [3] D. J. Zigrang and N. D. Sylvester. A review of explicit friction factor equations. *Journal of Energy Resources Technology, Transactions of the ASME*, 107(2):280–283, 1985, doi:10.1115/1.3231190.
- [4] J. Schumacher, A. Malhotra, K. Gräfe, and T. M. Buzug. Highly symmetric filter for a fully differential receive chain. *International Journal on Magnetic Particle Imaging*, 6(2):1–3, 2020, doi:10.18416/IJMPI.2020.2009031.

- [5] B. Zheng, P. W. Goodwill, N. Dixit, D. Xiao, W. Zhang, B. Gunel, K. Lu, G. C. Scott, and S. M. Conolly. Optimal Broadband Noise Matching to Inductive Sensors: Application to Magnetic Particle Imaging. *IEEE Transactions on Biomedical Circuits and Systems*, 11(5):1041–1052, 2017, doi:[10.1109/TBCAS.2017.2712566](https://doi.org/10.1109/TBCAS.2017.2712566).
- [6] M. Graeser, T. Knopp, P. Szwargulski, T. Friedrich, A. von Gladiss, M. Kaul, K. M. Krishnan, H. Ittrich, G. Adam, and T. M. Buzug. Towards Picogram Detection of Superparamagnetic Iron-Oxide Particles Using a Gradiometric Receive Coil. *Scientific Reports*, 7(1):6872, 2017, doi:[10.1038/s41598-017-06992-5](https://doi.org/10.1038/s41598-017-06992-5).